Supporting Information

Lawson et al. 10.1073/pnas.1107559108

SI Materials and Methods

Development of Mutant L188Q Surfactant Protein C (*SFTPC*) Mice. The plasmid containing mutant L188Q *SFTPC* was generated as previously described (1, 2). The L188Q *SFTPC* construct was cloned into the EcoRV site of a modified pBluescript II SK expression vector (pBSII KS/Asc). This vector contains a (tet-O)$_7$-CMV promoter together with bovine growth hormone polyadenylation sequences. The final plasmid, (tet-O)$_7$–L188Q *SFTPC*-myc–BGH.polyA, was verified by sequencing. A plasmid containing murine SFTPC.rtTA (mSFTPC.rtTA) was provided by E.E.M. To prevent basal leakiness, we used a third construct expressing a tetracycline-controlled transcriptional silencer (tTS) under control of the murine SFTPC promoter (3). We purified these three constructs with a GELase Agarose Gel-Digesting Preparation Kit (Epicentre) following the manufacturer's instructions, and these constructs were coinjected at the Vanderbilt Transgenic/ES Shared Resource facility to generate transgenic lines of mice (C57BL/6 background) with integration of all three constructs. Genotyping of founder animals was performed by Southern blot analysis, and later stages of genotyping were performed by PCR.

Transgenic mice expressing the reverse tetracycline transactivator (rtTA) under the human SFTPC promoter (hSFTPC.rtTA) were obtained from Jackson Laboratories. NF-κB/GFP/luciferase (NGL) mice, which have consensus NF-κB binding sites upstream of the HSV minimal thymidine kinase promoter driving the GFP/luciferase construct, have been described previously (4). All transgenic and WT mice for these experiments were in a C57BL/6J background and entered experiments at 8–10 wk of age. All mouse experiments were approved by the Vanderbilt Institutional Animal Care and Use Committee.

Antibodies. The following primary antibodies were used in these investigations: pro-SFTPC precursor protein (pro-SP-C) goat polyclonal antibody (Santa Cruz Biotechnology); S100A4 rabbit polyclonal antibody (obtained from Eric Neilson, Vanderbilt University); α-smooth muscle actin (αSMA) rabbit polyclonal antibody (Abcam); heavy-chain Ig binding protein (BiP) goal polyclonal antibody (Santa Cruz Biotechnology); X-box binding protein 1 (XBP1) rabbit polyclonal antibody (Santa Cruz); giantin rabbit polyclonal antibody (Abcam); myc mouse monoclonal antibody (Invitrogen Life Technologies); myc goat polyclonal antibody (Santa Cruz Biotechnology); active caspase-3 rabbit polyclonal antibody (Millipore); β-actin rabbit polyclonal antibody (Sigma); caspase-12 rabbit polyclonal antibody (Cell Signaling Technology); and CCAAT/enhancer-binding protein homologous transcription factor (CHOP) rabbit polyclonal antibody (Cell Signaling Technology).

Bleomycin Model. Bleomycin (0.04 unit; Bedford Laboratories) was injected intratracheally (i.t.) in WT and transgenic mice by using an intubation procedure as previously described (5). At baseline and at designated time points after bleomycin injection, lungs were harvested for histology, frozen tissue, bronchoalveolar lavage, or cell isolation as previously described (5–8).

Doxycycline (Dox) Administration. All L188Q *SFTPC* mice and controls were maintained on normal water ad libitum until transgene activation was desired. At that time, Dox (Sigma-Aldrich) was mixed in sterile water at a concentration of 2 g/dL with additional 2% sucrose. The bottles containing Dox were wrapped with foil to prevent light-induced Dox degradation, and Dox bottles were replaced twice per week.

Tunicamycin Administration. Tunicamycin (Sigma) was dissolved in DMSO and diluted to a concentration of 20 μg/mL in 20% DMSO diluted in PBS, and then 100 μL of solution was delivered to experimental mice by i.t. intubation. A similar volume of 20% DMSO diluted in PBS was used as a vehicle control.

Histology and Microscopy. Formalin-fixed, paraffin-embedded lung tissue was sectioned and stained with H&E or Masson's trichrome as previously described (7, 8). Light and fluorescent microscopy was performed with an Olympus IX81 Inverted Research Microscope configured with an Olympus IX2-DSU Biological Disk Scanning Unit.

Immunostaining. Immunohistochemistry (IHC) on paraffin-embedded lung tissue sections and immunocytochemistry on cell preparations were performed with primary antibodies and standard immunoperoxidase techniques as previously described (7, 8). Immunofluorescence staining was performed on cell preparations by using primary antibodies followed by appropriate fluorescent secondary antibodies (Jackson ImmunoResearch) with nuclear staining performed with DAPI using Vectashield mounting medium (Vector Laboratories) as previously described (5, 6).

TUNEL Assay. TUNEL assays on lung sections were performed as previously described (5, 8) with a commercially available kit (In Situ Cell Death Detection Kit; Roche Molecular Biochemicals) in accordance with the manufacturer's instructions. Counterstains for preparations were performed with hematoxylin.

Cell Culture/Isolation. Plasmids were transfected into A549 cells with an Effectene transfection kit (Qiagen) per the manufacturer's instructions. Cells were incubated with the transfection complexes under normal growth conditions for 4 h, and then 0.5–1.0 μg/mL Dox was added to the medium for induction of transgene expression. After transient transfection for 24 h, cells were harvested for determination of gene expression by Western blot analysis. Type II alveolar epithelial cells (AECs) were isolated from adult mice using techniques as previously described (6, 7).

Lung Lavage and Cell Counts. Bronchoalveolar lavage was performed as detailed previously (5, 8). After euthanasia, three 800-μL lavages of sterile saline were performed with a 20-gauge blunt-tipped needle inserted into the trachea. Samples were centrifuged at 400 × *g* for 10 min, and cells were resuspended and counted manually under light microscopy with a hemocytometer. Approximately 30,000 cells from each specimen were loaded onto slides using a Cytospin 2 centrifuge (Shandon Southern Products). These slide preparations were then stained with a modified Wright stain.

RNA Isolation, Real-Time RT-PCR, and Densitometry. Total RNA from type II AECs and lung tissue was isolated by using the RNeasy Mini Kit (Qiagen), according to the manufacturer's specifications. To remove contaminating genomic DNA, samples were incubated with DNase (Ambion) and then converted to cDNA using SuperScript II reverse transcriptase (Invitrogen). For BiP evaluation, PCR amplification and quantification were performed with SYBR Green PCR Master Mix (Ambion). Primer sequences were as follows: BiP (forward, 5′-CCT GCG TCG GTG TGT TCA AG-3′; reverse, 5′-AAG GGT CAT TCC AAG TGC G-3′) and RPL19

(forward, 5′-ATG CCA ACT CCC GTC AGC AG -3′; reverse, 5′-TCA TCC TTC TCA TCC AGG TCA CC-3′). PCR amplification was conducted on a StepOnePlus Real-Time PCR System (Applied Biosystems). The relative mRNA amount in each sample was calculated based on its threshold cycle (C_t) in comparison with the C_t of the housekeeping gene *RPL19*. Relative mRNA expression was presented as $2^{\Delta Ct(\text{housekeeping gene})-\Delta Ct(\text{target gene})}$. Evaluation of XBP1 splicing was performed by using previously described methods (9). Primer sequences for XBP1 were as follows: forward, 5′-CTG GAA AGC AAG TGG TAG A-3′ and reverse, 5′-CTG GGT CCT TCT GGG TAG AC-3′. cDNA (2 μL) was used with a reaction volume of 50 μL. PCR products were run on a 2.5% gel with 398-bp and 424-bp forms representing spliced and unspliced fragments, respectively. XBP1 splicing ratio was calculated as spliced divided by total. Densitometry was performed with NIH Image J software where band densities were calculated and subtracted from the background.

For *SFTPC* expression, real-time reactions were performed on a Bio-Rad iCycler with iQ SYBR Green Supermix (Bio-Rad). Standard curves were generated by the amplification of target sequences previously cloned into pGEM-T (Promega), in dilution series from 10^{-1} to 10^{-6} fmol of target sequence per well. Real-time PCR primers for mutant L188Q *SFTPC* were as follows: 5′ (located in the inserted Myc sequence), 5′-GAG CAG AAA CTC ATC TCT G-3′ and 3′ (located in the mSFTPC sequence), 5′-CTG GCT TGT AGG CGA TCA GC-3′. Real-time PCR primers for mouse native *SFTPC* are as follows: sense, 5′-CTC CAC ACC CAC CTC TAA GCT-3′ and antisense, 5′-GTA GGA GAG ACA CCT TTC CTT-3′.

Western Blot Analysis. Western blot analysis was performed on cytoplasmic extracts from whole-lung and cell preparations by using previously described techniques (7).

In Vivo Bioluminescence and Luciferase Measurements. Live-animal bioluminescence imaging in NGL transgenic mice was performed after i.p. injection of luciferin (1 mg per mouse in 100 μL of isotonic saline) using an intensified CCD camera (IVIS 200; Xenogen) as previously described (4). Whole-lung tissue luciferase levels were determined as previously described (4).

Measurement of Airway Resistance and Compliance. For airway resistance and compliance measurements, mice were anesthetized with i.p. pentobarbital, and tracheas were cannulated with a 20-gauge metal stub adapter. Each mouse was placed on a small-animal ventilator, flexiVent (SCIREQ), with 150 breaths per min and a tidal volume of 10 mL/kg of body weight. Airway resistance and static lung compliance (using a 2-s breath pause) were assessed with SCIREQ manufacturer-provided software, which calculates the resistance by dividing the change in pressure by the change in flow (cm of H_2O/mL per s) and compliance by dividing change in volume by change in pressure (mL/cm of H_2O).

Semiquantitative Scoring. Quantification of lung fibrosis on histological specimens was performed by an investigator blinded to the group using a semiquantitative score on 10 sequential, nonoverlapping fields (magnification: ×300) as previously described (5, 8). For scoring of S100A4+ and αSMA+ lung fibroblasts, slides immunostained for S100A4 or αSMA were evaluated on a 0- to 4-point scale as previously described (8): 0, no positive cells; 1, few (≤3) positive cells; 2, multiple (>3) individual positive cells; 3, multiple positive cells in isolated clumps; and 4, multiple clumps of positive cells. The mean score for the 10 sequential fields represented the score for each individual specimen. For evaluation of TUNEL staining, slides were evaluated on 10 sequential, nonoverlapping fields (magnification: ×600) of lung parenchyma for each specimen and were scored using a 0- to 4-point semiquantitative scale as previously described: 0, no positive cells; 1, ≤1% of cells in field positive; 2, 1–5% of cells in field positive; 3, 5–10% of cells in field positive; and 4, 10–25% of cells in field positive (10).

Collagen Content. Frozen lung tissue samples were hydrolyzed in 6 M HCl, and hydroxyproline content was quantitated by using a microplate assay based on Ehrlich's reaction as previously described (11). Lung collagen content was calculated from these results as hydroxyproline accounts for ∼13.3% of collagen by weight.

Statistics. Statistical analyses were performed with GraphPad InStat (GraphPad Software). Differences among groups were assessed with one-way ANOVA. Differences between pairs were assessed with Student's *t* test. Results are presented as mean ± SEM. *P* values <0.05 were considered significant.

1. Thomas AQ, et al. (2002) Heterozygosity for a surfactant protein C gene mutation associated with usual interstitial pneumonitis and cellular nonspecific interstitial pneumonitis in one kindred. *Am J Respir Crit Care Med* 165:1322–1328.
2. Lawson WE, et al. (2008) Endoplasmic reticulum stress in alveolar epithelial cells is prominent in IPF: Association with altered surfactant protein processing and herpesvirus infection. *Am J Physiol Lung Cell Mol Physiol* 294:L1119–L1126.
3. Zhu Z, Ma B, Homer RJ, Zheng T, Elias JA (2001) Use of the tetracycline-controlled transcriptional silencer (tTS) to eliminate transgene leak in inducible overexpression transgenic mice. *J Biol Chem* 276:25222–25229.
4. Everhart MB, et al. (2006) Duration and intensity of NF-&kappaB activity determine the severity of endotoxin-induced acute lung injury. *J Immunol* 176:4995–5005.
5. Degryse AL, et al. (2010) Repetitive intratracheal bleomycin models several features of idiopathic pulmonary fibrosis. *Am J Physiol Lung Cell Mol Physiol* 299:L442–L452.
6. Tanjore H, et al. (2009) Contribution of epithelial-derived fibroblasts to bleomycin-induced lung fibrosis. *Am J Respir Crit Care Med* 180:657–665.
7. Lawson WE, et al. (2005) Characterization of fibroblast-specific protein 1 in pulmonary fibrosis. *Am J Respir Crit Care Med* 171:899–907.
8. Lawson WE, et al. (2005) Increased and prolonged pulmonary fibrosis in surfactant protein C-deficient mice following intratracheal bleomycin. *Am J Pathol* 167: 1267–1277.
9. Shang J (2005) Quantitative measurement of events in the mammalian unfolded protein response. *Methods* 35:390–394.
10. Cheng DS, et al. (2007) Airway epithelium controls lung inflammation and injury through the NF-&kappaB pathway. *J Immunol* 178:6504–6513.
11. Brown S, Worsfold M, Sharp C (2001) Microplate assay for the measurement of hydroxyproline in acid-hydrolyzed tissue samples. *Biotechniques* 30:38–40, 42.

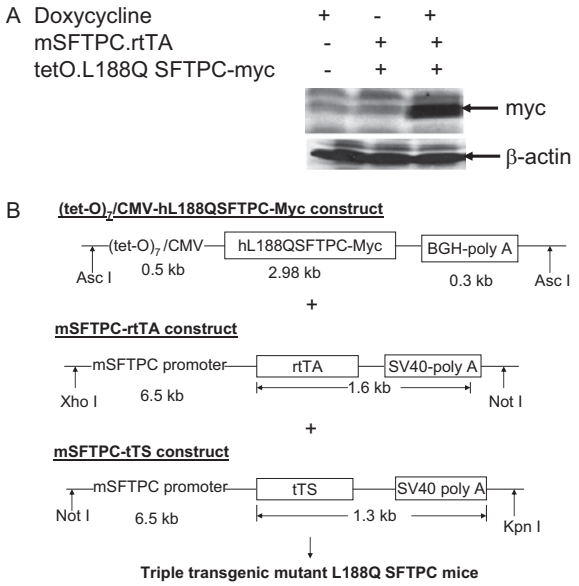

Fig. S1. Constructs were developed to express myc-tagged mutant L188Q *SFTPC* in a tetracycline-dependent fashion. (*A*) Western blot analysis for the myc-tagged transgene in A549 cells transfected with both the mSFTPC.rtTA and tetO.L188Q *SFTPC*-myc constructs. β-Actin is shown as a loading control. (*B*) Schematic of rtTA, tTS, and L188Q myc-tagged *SFTPC* constructs that were designed for the purpose of generating the transgenic L188Q *SFTPC* mouse.

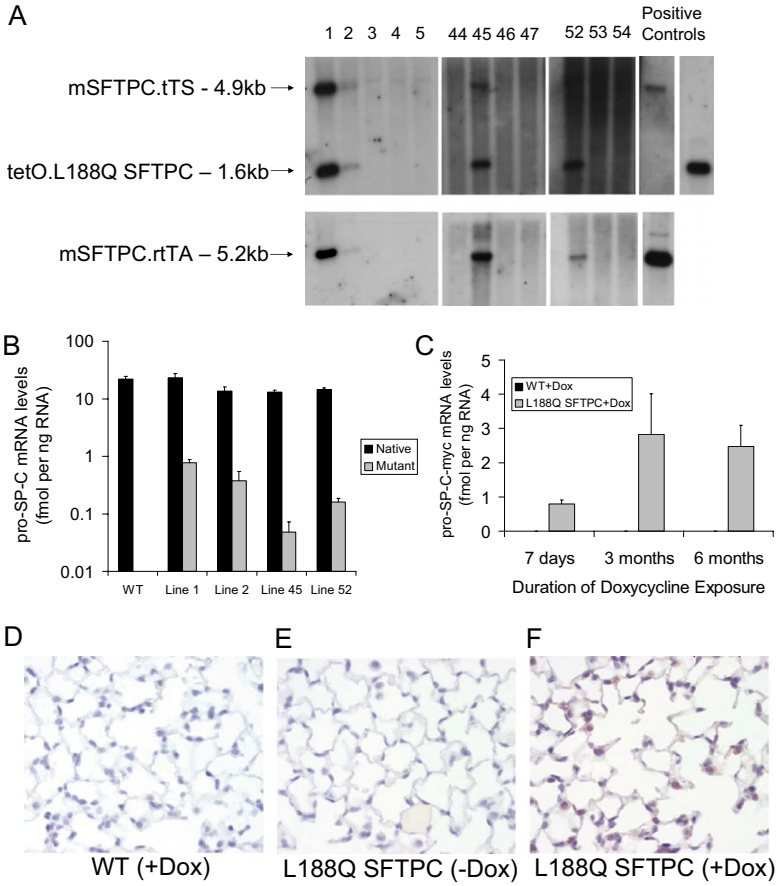

Fig. S2. Expression of mutant pro-SP-C is detected in vivo in L188Q *SFTPC* mice. (*A*) Southern blot analysis for the three transgenic constructs demonstrating identification of four founder lines: 1, 2, 45, and 52. (*B*) pro-SP-C–myc mRNA levels for native versus mutant pro-SP-C for each founder line exposed to Dox for 1 wk. (n = 3 per group.) (*C*) pro-SP-C–myc mRNA levels in whole lung from founder line 1 mice exposed to Dox for up to 6 mo. (n = 3 per group.) Graphical data are presented as mean ± SEM. (*D–F*) IHC for myc tag in WT mice with Dox (*D*) and L188Q *SFTPC* mice without Dox (*E*) and with Dox (*F*). (Magnification: ×400.)

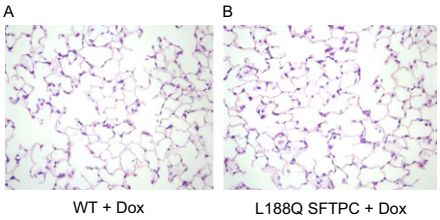

Fig. S3. Expression of mutant L188Q *SFTPC* in vivo does not lead to aberrant lung histology. H&E-stained lung tissue sections from WT (*A*) and L188Q *SFTPC* (*B*) mice exposed to Dox for 6 mo. (Magnification: ×200.)

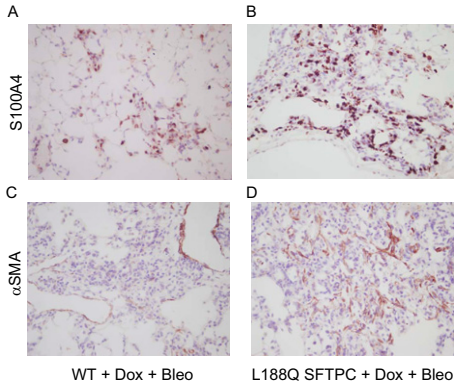

Fig. S4. Mice expressing mutant L188Q *SFTPC* had more lung fibroblasts after i.t. bleomycin (Bleo) than littermate controls did. (*A* and *B*) IHC for the fibroblast marker S100A4 in lung sections from WT (*A*) and L188Q *SFTPC* (*B*) mice at 3 wk after bleomycin treatment. (*C* and *D*) IHC for the myofibroblast marker αSMA in lung sections from WT (*C*) and L188Q *SFTPC* (*D*) mice at 3 wk after bleomycin treatment. (Magnification: ×200.)

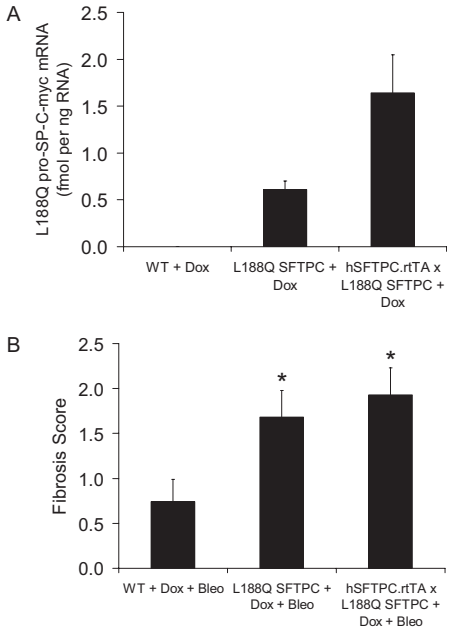

Fig. S5. Crossing L188Q *SFTPC* mice to the human *SFTPC* promoter-driven rtTA (h*SFTPC*.rtTA) did not alter lung fibrosis. (*A*) L188Q pro-SP-C–myc mRNA levels in whole-lung tissue from WT, L188Q *SFTPC*, and h*SFTPC*.rtTA × L188Q *SFTPC* mice exposed to Dox for 1 wk. (n = 3 per group.) (*B*) Semiquantitative fibrosis scoring of trichrome-stained lung sections from WT, L188Q *SFTPC*, and h*SFTPC*.rtTA × L188Q *SFTPC* mice at 3 wk after 0.04 unit of i.t. bleomycin (Bleo). (n = 5–7 per group; $^*P < 0.05$ compared with WT.) Graphical data are presented as mean ± SEM.

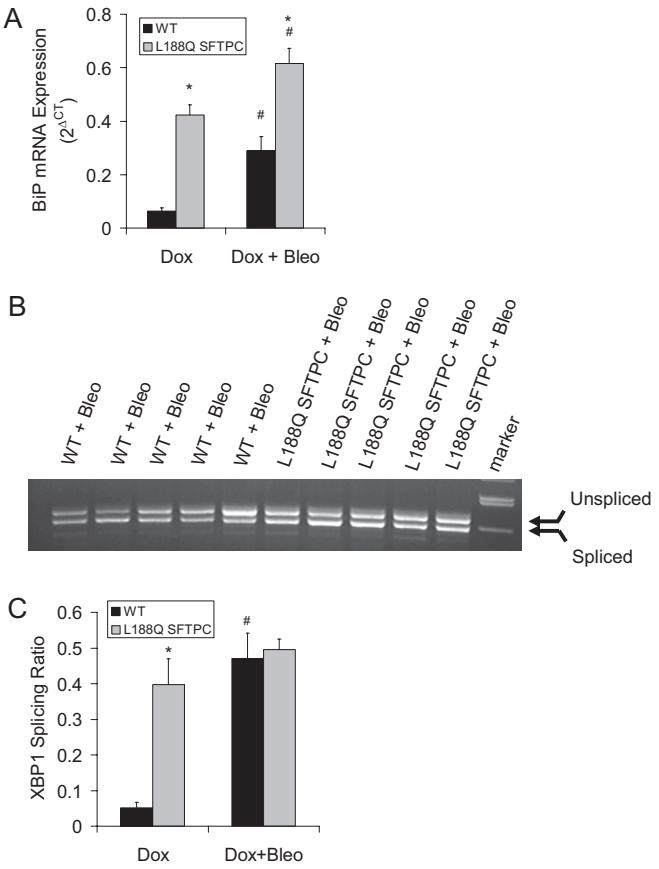

Fig. S6. Markers of endoplasmic reticulum (ER) stress are increased by bleomycin (Bleo) treatment in WT mice and mutant L188Q *SFTPC* mice. (*A*) Real-time RT-PCR for expression of BiP mRNA normalized to expression of the housekeeping gene *RPL19* at 1 wk after bleomycin treatment. (n = 4–5 per column; $^{*}P < 0.001$ for WT versus L188Q *SFTPC* in both Dox and Dox + Bleo groups; $^{\#}P < 0.05$ for Dox versus Dox + Bleo for both WT and L188Q *SFTPC*.) (*B*) RT-PCR gel demonstrating splice variants for XBP1 mRNA in lungs of WT and L188Q *SFTPC* mice treated with Dox and harvested 1 wk after bleomycin injection. (*C*) XBP1 splicing analysis by densitometry. (n = 5 per column; $^{*}P < 0.01$ for WT versus L188Q *SFTPC* in Dox group; $^{\#}P < 0.001$ for Dox versus Dox + Bleo for WT.) Graphical data are presented as mean ± SEM.

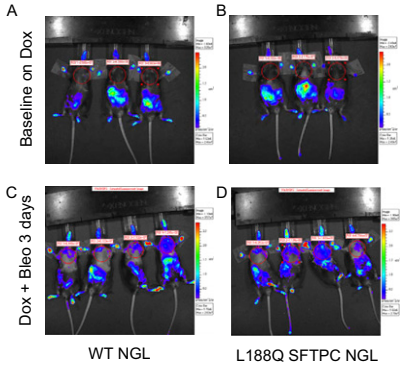

Fig. S7. (*A* and *B*) Representative in vivo photon-capture images from WT/NGL (*A*) and L188Q *SFTPC*/NGL (*B*) mice after 14 d of Dox treatment. (*C* and *D*) Representative in vivo photon-capture images from WT/NGL (*C*) and L188Q *SFTPC*/NGL (*D*) mice at 3 d after i.t. bleomycin (Bleo) with continued Dox.

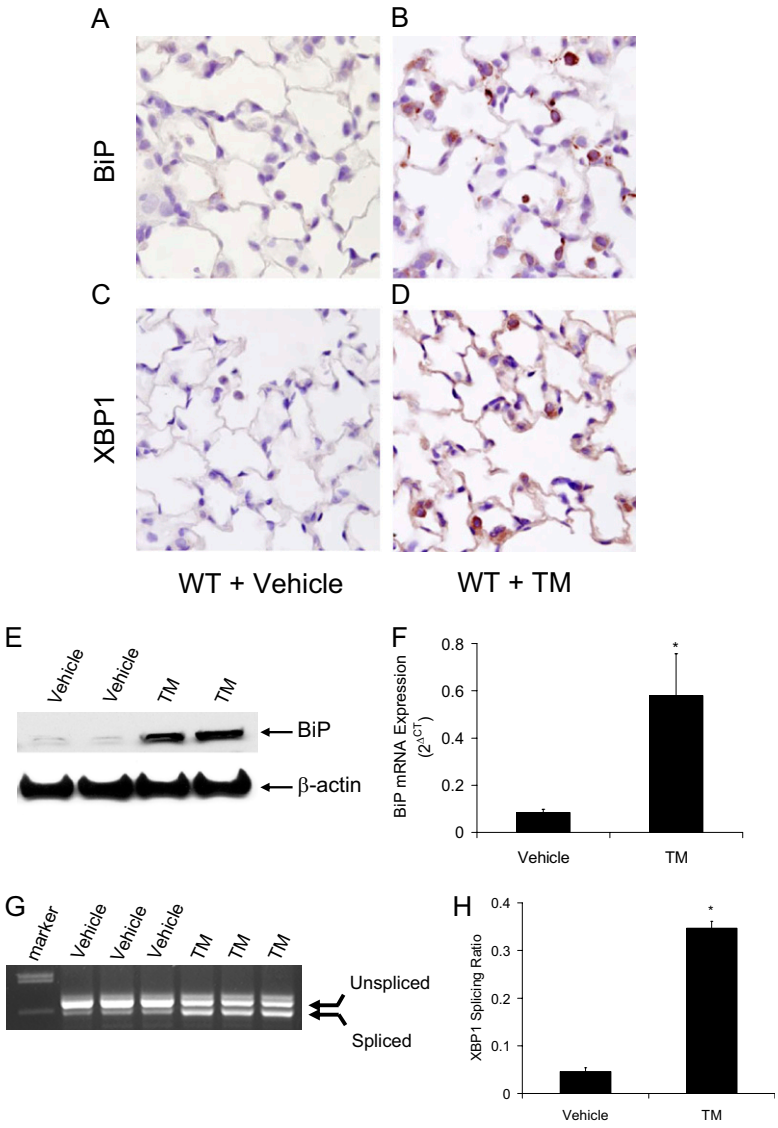

Fig. S8. Tunicamycin (TM) leads to ER stress in the lungs. (*A* and *B*) IHC for the ER stress marker BiP in lung sections from WT mice at 48 h after i.t. administration of vehicle (DMSO; *A*) and tunicamycin (*B*). (*C* and *D*) IHC for the ER stress marker XBP1. (Magnification: ×600.) (*E*) Western blot analysis for BiP using whole-lung lysates from WT mice at 48 h after i.t. administration of vehicle or tunicamycin. β-Actin is shown as loading control. (*F*) Real-time RT-PCR for expression of BiP mRNA normalized to expression of the housekeeping gene *RPL19*. (n = 3 per column; $^*P < 0.05$ between columns.) (*G*) RT-PCR gel demonstrating splice variants for XBP1 mRNA in lungs of WT mice treated with either vehicle or tunicamycin. (*H*) XBP1 splicing analysis by densitometry. (n = 3 per column; $^*P < 0.0001$ between columns.) Graphical data are presented as mean ± SEM.